https://doi.org/10.5194/egusphere-2026-4150
Preprint. Discussion started: 16 July 2026

Low-Frequency Stratospheric Variability and its Link to Surface Climate: Insights from Reanalysis and Multi-Century Coupled Climate Model Simulations

Liping Wang[1,2,*], Gang Chen[3], Xiuyuan Ding[3], Haijun Yang[4], and Daniela I.V. Domeisen[1,5]

[1]Faculty of Geosciences and Environment, University of Lausanne, Lausanne, Switzerland
[2]Department of Atmospheric and Oceanic Sciences, School of Physics, Peking University, China
[3]Department of Atmospheric and Oceanic Sciences, University of California, Los Angeles, CA, USA
[4]Department of Atmospheric and Oceanic Sciences, Fudan University, Shanghai, China
[5]Institute for Atmospheric and Climate Science, ETH Zurich, Zurich, Switzerland
[*]now at: Department of Environmental Sciences, University of Virginia, Charlottesville, VA, USA

Correspondence: Liping Wang (lpwang7@pku.edu.cn; lpwang736@gmail.com)

Abstract. The Northern Hemisphere stratosphere exhibits variability across subseasonal to multi-decadal timescales. While subseasonal-to-seasonal stratospheric variations have been shown to link to surface climate variability, low-frequency stratospheric variability and its coupling to the surface remain less well understood due to the short observational record and model limitations in simulating variability on these timescales. Here, we analyze low-frequency stratospheric variability using the CERA-20C Reanalysis, and multi-century simulations from three fully coupled models: CESM2.0-WACCM, CESM1.0-CAM4 and CESM2.0-CAM6. We identify an oscillatory stratospheric variability with a ∼15-year period that is consistently present across reanalysis and all three models. Wavelet analysis suggests that this ∼15-year periodicity is highly non-stationary and intermittent owing to the coexistence of other periodic variability on longer timescales. The ∼15-year frequency peak in stratospheric variability is closely associated with the North Atlantic Oscillation (NAO) and tends to lead NAO surface variability. Although all models simulate the stratospheric ∼15-year peak to some degree, they differ in simulating the link between this frequency peak and the surface NAO: WACCM shows the closest agreement with reanalysis, whereas CAM4 demonstrates limited capability in simulating low-frequency stratosphere-NAO coupling, and CAM6 again exhibits closer agreement with reanalysis. By contrast, the relationship between the stratospheric ∼15-year variability and the Aleutian Low is comparatively weak and less consistent across the reanalysis and models. These results help improve our understanding of how low-frequency stratospheric variability is connected to surface variability.

1 Introduction

The extratropical stratosphere exhibits variability on a wide range of timescales from daily variability to long-term trends. Reanalyses suggest multi-decadal weakening and an equatorward shift of the Arctic stratospheric polar vortex, although these trends may largely reflect internal variability (Seviour, 2017), while future projections show large model uncertainty in long-term changes in vortex strength (Karpechko et al., 2022). One of the most prominent examples of stratospheric dynamical

https://doi.org/10.5194/egusphere-2026-4150
Preprint. Discussion started: 16 July 2026

variability are sudden stratospheric warming events (SSWs) (Baldwin et al., 2021), which are associated with a reversal of the typical westerly zonal-mean zonal winds in the winter polar stratosphere, and can subsequently impact surface weather (Baldwin and Dunkerton, 2001). These events are therefore one of the prime examples for inducing stratosphere - troposphere coupling in the extratropics. Observational records show that SSWs in the Northern Hemisphere occur around six times per decade (Charlton and Polvani, 2007), but their frequency also exhibits pronounced decadal variability. For instance, almost no SSWs were detected in the 1990s, whereas the 1980s and 2000s saw a higher number of such events (Butler et al., 2015; Domeisen, 2019; Pawson and Naujokat, 1999; Manney et al., 2005). Understanding the variability of the stratosphere is essential for predicting and projecting surface weather and climate (Domeisen and Butler, 2020; Domeisen et al., 2019; Kidston et al., 2015; Simpson et al., 2018; Karpechko et al., 2022). A wide range of studies have examined the link between the stratosphere and surface anomalies on daily to seasonal timescales (Bett et al., 2023; Domeisen, 2019; Domeisen et al., 2020; Ding et al., 2022, 2023; Wang and Chen, 2010; Chen and Ding, 2026; Shen et al., 2023). However, due to the short observational record and the limited availability of long-term coupled ocean-atmosphere model simulations, low-frequency stratospheric variability and its interaction with surface climate are less well understood.

Several studies have explored the origins and impacts of extratropical stratospheric multi-year to multi-decadal variability, suggesting that it may arise from external forcing or internal variability. Kodera and Kuroda (2002) suggested that long-term stratospheric variability is driven by the 11-year solar cycle, which can modulate the variation in the polar vortex through planetary waves. Seviour (2017) analyzed two reanalysis datasets from 1980 to 2016, finding that stratospheric polar vortex variability is most likely a result of internally generated variability. Using a multi-century General Circulation Model (GCM) simulation, Schimanke et al. (2011) noted a 52-year period of stratospheric variability and found that Eurasian snow cover, blocking, and Atlantic sea surface temperature (SST) vary in-phase with a similar timescale of approximately 52 years. Dimdore-Miles et al. (2021) linked the 90-year variability in SSWs to multi-decadal variability in the amplitude of the tropical stratospheric quasi-biennial oscillation (QBO) through the Holton–Tan relationship in a 1000-year high-top UK Earth System Model (UKESM) simulation. Butler et al. (2023) used three large-ensemble coupled model simulations over the period 1850-2100 and found that stratosphere-troposphere coupling amplifies decadal variability of extratropical surface temperatures. Future uncertainty in the stratospheric polar vortex response to climate change may also contribute to model spread in tropospheric circulation change (Simpson et al., 2018)

Low-frequency stratospheric variability has been linked to North Pacific and North Atlantic surface variability (Manzini et al., 2012; Omrani et al., 2014). Using reanalysis datasets and short numerical simulations, the North Pacific circulation, such as the Aleutian Low, the Pacific Decadal Oscillation (PDO) (Hu and Guan, 2018; Ayarzagüena et al., 2021; Kren et al., 2016) and the North Pacific Gyre Oscillation (NPGO) (Li et al., 2018) are suggested to impact the stratosphere on multi-year to multi-decadal timescales by modifying the upward propagation of planetary waves into the stratosphere. Over the North Atlantic, the low-frequency stratospheric variability is found to have a downward impact on the NAO and the Atlantic Meridional Overturning Circulation (AMOC). Using a 4000-year simulation with the low-top GFDL-CM2.1 model, Reichler et al. (2012) demonstrated that the AMOC exhibits a delayed oscillatory response to low-frequency variations in the stratospheric polar vortex. Dimdore-Miles et al. (2022) further studied the mechanism of this stratosphere-AMOC teleconnection on decadal-

https://doi.org/10.5194/egusphere-2026-4150
Preprint. Discussion started: 16 July 2026

to-multi-decadal timescales. The main process they found is that long-lived stratospheric vortex events can modulate NAO anomalies, which further impact the heat flux and SSTs over the North Atlantic, thus triggering decadal-to-multi-decadal variability in the deeper ocean circulation. This stratosphere-troposphere-Atlantic decadal-to-multi-decadal oscillation coupling was also found in the Max Planck Institute Earth System Model (Omrani et al., 2022).

However, current research on low-frequency stratospheric variability and its coupling with the troposphere still faces several challenges. Firstly, numerous previous studies have aimed to clarify the low-frequency coupling between the stratosphere and surface circulation by primarily focusing on short-term observational changes that may cause large uncertainty and low statistical significance. Secondly, previous research has generally used relatively short and single simulations due to the limited availability of long-term stratosphere-resolving model simulations. Moreover, few studies have systematically compared reanalysis with multiple model simulations to identify low-frequency signals that are consistently present in both observations and models. In this study, we analyze the CERA-20C reanalysis for 1900-2010, together with three multi-century simulations from the NCAR Community Earth System Model (CESM). CESM is one of the most widely-used fully coupled global climate model family that provides both stratosphere-resolving (high-top) and non-stratosphere-resolving (low-top) configurations, enabling long integrations suitable for studying stratospheric low-frequency variability. The high-top component WACCM (the Whole Atmosphere Community Climate Model Version 6) is particularly effective at representing stratospheric dynamics and stratosphere–troposphere coupling (Gettelman et al., 2019), and therefore provides a useful framework for examining stratospheric variability. For comparison, we also analyze two low-top configurations: CAM4 (the Community Atmosphere Model, version 4) integrated for 1000 years and CAM6 (the Community Atmosphere Model, version 6) integrated for 2000 years.

The aim of this work is to address the following three questions: (1) What spectral peaks characterize long-term variability of the stratospheric polar vortex in reanalysis and climate models? (2) How is stratospheric long-term variability linked to tropospheric circulation variability? (3) How do low-top and high-top models differ in their representation of stratospheric long-term variability and its coupling to the troposphere?

2 Data and Methods

2.1 Reanalysis and model data

For examining the low-frequency stratospheric variability we start by using the CERA-20C reanalysis covering the period 1900-2010. CERA-20C is the ECMWF coupled atmosphere-ocean reanalysis for the twentieth century, providing a 10-member ensemble of reanalysis to account for observational and model errors (Laloyaux et al., 2018). It contains 91 vertical levels between the surface and 0.01 hPa in the atmosphere, with a horizontal resolution of 125 km. The ocean has a roughly 110 km horizontal resolution with meridional refinement at the equator and 42 vertical levels. The details are listed in Table 1.

Although this reanalysis product covers a longer period than most other such products, it is still short for analyzing multi-decadal variability. Hence, we also use climate model output from three long-term model simulations from the CESM. CESM is a fully-coupled global climate model, providing state-of-the-art simulations of Earth's past, present, and future climate states (http://www2.cesm.ucar.edu/). For the atmospheric component, WACCM from CESM2.0 uses a nominal 1° resolution (0.9°in

https://doi.org/10.5194/egusphere-2026-4150
Preprint. Discussion started: 16 July 2026

Datasets	Vertical resolution (top model level)	Horizontal resolution	Length
CERA-20C	91 levels (0.01 hPa)	125 km	110 years
CESM1.0-CAM4	26 levels (3.54 hPa)	3.75°×3.75°	1000 years
CESM2.0-CAM6	32 levels (2.25 hPa)	0.9°×1.25°	2000 years
CESM2.0-WACCM	66 levels (0.01 hPa)	0.9°×1.25°	500 years

Table 1. List of reanalysis and model simulations used in this study.

latitude and 1.25° in longitude), with 66 vertical levels and a model top at 0.01 hPa (Danabasoglu et al., 2020). CAM6 from CESM2.0 has the same horizontal grid as WACCM, except that it uses 32 vertical levels with a relatively low model top level of 2.25 hPa. CAM4 from CESM1.0 uses 26 vertical levels up to 3.54 hPa and a horizontal resolution of about $3.75° \times 3.75°$. Compared to stratosphere-resolving high-top models usually used for stratospheric analysis such as WACCM, CAM6 and CAM4 have a lower model top and are thus referred to as low-top models. For the ocean component, CESM1.0 uses the Parallel Ocean Program Version 2 (POP2). It contains 60 vertical levels and runs at a uniform resolution of 3.6° in the zonal direction. The resolution in the meridional direction is non-uniform: it is 0.6° at the equator, gradually increases to a maximum of 3.4° at 35°N/S, and then decreases poleward. The CESM2.0 ocean component is the same as in CESM1.0, but with higher horizontal resolution, using 1.125° in the zonal direction. The resolution varies significantly in the meridional direction, with the highest resolution of 0.27° at the equator. In the Southern Hemisphere, the resolution steadily increases, peaking at 0.53° at 32°S before stabilizing further southward. In the Northern Hemisphere, the resolution increases northward, with the highest resolution of 0.38° in the northwestern Atlantic Ocean and the coarsest resolution of 0.64° in the northwestern Pacific Ocean. All the model control runs are forced using Coupled Model Intercomparison Project Phase (CMIP) preindustrial conditions from the 1850s, with a CO_2 level of 285 ppm. CESM1.0-CAM4 is integrated for 2600 years, and we analyze the last 1000 years. CESM2.0-WACCM and CESM2.0-CAM6 are integrated for 500 and 2000 years, respectively. Both simulations are from the NCAR CESM2.0 preindustrial control experiments (Danabasoglu et al., 2020) and are in quasi-equilibrium throughout the integrations. The output is given as monthly mean data.

To examine model biases in representing the stratospheric polar vortex, we compare the climatological 10 hPa geopotential height and its zonal wave-1 and wave-2 components with CERA-20C reanalysis (Figure A1). The 10 hPa geopotential height reflects the strength of the polar vortex, while its wave-1 and wave-2 components characterize the planetary-scale structure of the vortex. The high-top model WACCM simulates a vortex structure and strength broadly consistent with the CERA-20C reanalysis, whereas the low-top models CAM4 and CAM6 exhibit a stronger polar vortex than reanalysis. All three models reasonably reproduce the observed wave-1 and wave-2 spatial patterns. CAM6 simulates wave amplitudes comparable to CERA-20C, while WACCM simulates slightly reduced amplitudes. In contrast, CAM4 produces a stronger wave-1 amplitude, particularly over the Eurasian sector, and a substantially weaker wave-2 amplitude relative to reanalysis.

https://doi.org/10.5194/egusphere-2026-4150
Preprint. Discussion started: 16 July 2026

2.2 Data diagnostics

The strength of the stratospheric polar vortex is defined as the standardized first principal component (PC) of the empirical orthogonal function (EOF) of the zonal mean deseasonalised 10 hPa geopotential height north of 20°N during boreal winter (November-March), termed the *Northern Hemisphere Annular Mode (NAM) Index* (Thompson and Wallace, 2001). The North Atlantic Oscillation (NAO) index is defined as the first PC of the EOF of the November-March mean sea level pressure in the North Atlantic basin (20°N-80°N, 90°W-40°E) (Feldstein and Franzke, 2006; Domeisen et al., 2018; Hurrell et al., 2001). The Aleutian Low index is calculated as the first PC of the EOF of the November-March mean sea level pressure in the North Pacific basin (20°N-80°N, 120°E-120°W) (Linkin and Nigam, 2008; Yu and Kim, 2011). The Pacific decadal oscillation (PDO) index is the leading EOF pattern of the November-March mean sea surface temperature (SST) anomalies in the North Pacific basin (20°N-80°N, 120°E-120°W) (Lorenzo et al., 2023; Mantua et al., 1997). All indices are obtained by removing the seasonal cycle and the linear trend, and are then normalized.

We perform regression analysis between the stratospheric index and the surface circulation indices for a range of time lags between the predictor and predictand. The lead-lag regression is defined as follows:

$$\text{Surface indices}(t+\Delta t) = r \times \text{stratospheric NAM index}(t) \tag{1}$$

where t is a specific point in time, r is the regression coefficient between surface indices and stratospheric NAM index. The time interval $\Delta t > 0$ ($\Delta t < 0$) indicates that the stratospheric polar vortex leads (lags) the surface circulation by $|\Delta t|$ years. For example, $\Delta t = 10$ indicates that the stratospheric polar vortex leads the surface circulation by 10 years. By contrast, $\Delta t = -10$ indicates the surface circulation leads the stratospheric polar vortex by 10 years. $\Delta t = 0$ indicates an instantaneous regression between the stratospheric polar vortex and the surface circulation.

2.3 Wavelet analysis

Wavelet analysis is a widely used tool for examining time series with non-stationary spectral power, enabling the identification of dominant variability modes and their temporal evolution. This method has been extensively applied to study the low-frequency variability of the climate system, such as the El Niño-Southern Oscillation (ENSO; Torrence and Compo (1998)), the Madden-Julian oscillation (MJO; Whitcher et al. (2000)) and regional precipitation (Nalley et al., 2019; Coulibaly and Burn, 2004). Given that the time series of the stratospheric polar vortex displays multiple variability periods (Dimdore-Miles et al., 2021, 2022), we employ wavelet analysis based on Torrence and Compo (1998) to examine the low-frequency variability of the stratosphere.

The continuous wavelet transform of a one-dimensional time series $x(t)$ (t=1,2$\cdots$N) is given by the convolution between the series and a wavelet function ψ.

$$W_n(s) = \sum_{n'=0}^{N} x_{n'}(t)\psi^* \left[\frac{(n'-n)\Delta t}{s}\right] \tag{2}$$

https://doi.org/10.5194/egusphere-2026-4150
Preprint. Discussion started: 16 July 2026

where s, n and Δt are the wavelet scale, time index and uniform time step, respectively. n' is the location where the wavelet transform is applied. ψ^* denotes the complex conjugate of the wavelet function ψ. $|W_n(s)|^2$ is the wavelet power spectrum, indicating the distribution of signal power across different time scales. The wavelet power spectrum provides insights into the dominant frequencies present in the time series and how they evolve over time.

We here choose the Morlet wavelet because it provides a good balance between time and frequency localizations (Grinsted et al., 2004), thus can effectively reflect the oscillatory features of the stratospheric polar vortex time series. The Morlet wavelet function is defined as

$$\psi(t) = \pi^{-\frac{1}{4}} e^{i\omega_0 t} e^{-t^2/2} \tag{3}$$

where ω_0 and t are the non-dimensional central frequency and the non-dimensional time parameter, respectively. $\psi(t)$is the Morlet wavelet function, used to transform a time series into frequency components.

3 Results

3.1 Low-frequency stratospheric variability periods

We begin by examining the low-frequency variability of the stratospheric polar vortex using power spectral analysis (Figure 1). To better identify low-frequency signals, the NAM index is smoothed using a Gaussian filter (σ = 2 years) following the method in Reichler et al. (2012) and Dimdore-Miles et al. (2022). Because the model integrations have different lengths (see Table 1), we compute spectra from 250-year segments for each simulation and then average across segments to obtain a consistent estimate of spectral power. The CERA-20C ensemble mean (Figure 1a, red solid line) exhibits a statistically significant peak near 15 years that exceeds the 95% confidence level (black dashed line), and all 10 members (grey solid lines) also show enhanced power around this ∼15-year period. Importantly, the same ∼15-year peak is present in all three CESM simulations. In addition to the dominant ∼15-year peak, three CESM simulations show enhanced power at lower frequencies near 30 years. A comparable ∼30-year peak has also been reported in another high-top model, UKESM (Figure 7d in Dimdore-Miles et al. (2022)). Although some CERA-20C members display peaks around 20-30 years, the considerable model spread underscores the challenge of effectively analyzing the ∼30-year frequency peak due to the limited length of the observational record. Therefore, in this study, we mainly focus on the ∼15-year peak, which is consistently evident in both reanalysis and model simulations in Section 3.2. We will briefly discuss the potential ∼30-year peak in model simulations in Section 3.3.

We further use wavelet analysis to examine the low-frequency signals in the stratospheric NAM index (Figure 2), given the non-stationary spectral characteristics of the stratospheric polar vortex time series (Dimdore-Miles et al., 2021). Consistent with the results shown in power spectrum (Figure 1), the CERA-20C wavelet spectrum exhibits a significant power signal around 15 years that persists for nearly four decades (Figure 2a). In three model simulations, the wavelet spectrum displays non-stationary power over several frequencies. The WACCM wavelet spectrum shows a relatively continuous power during 10–40 years, with the most significant peak in power near 30-40 years of periodicity occurring during model years 150-250,

https://doi.org/10.5194/egusphere-2026-4150
Preprint. Discussion started: 16 July 2026

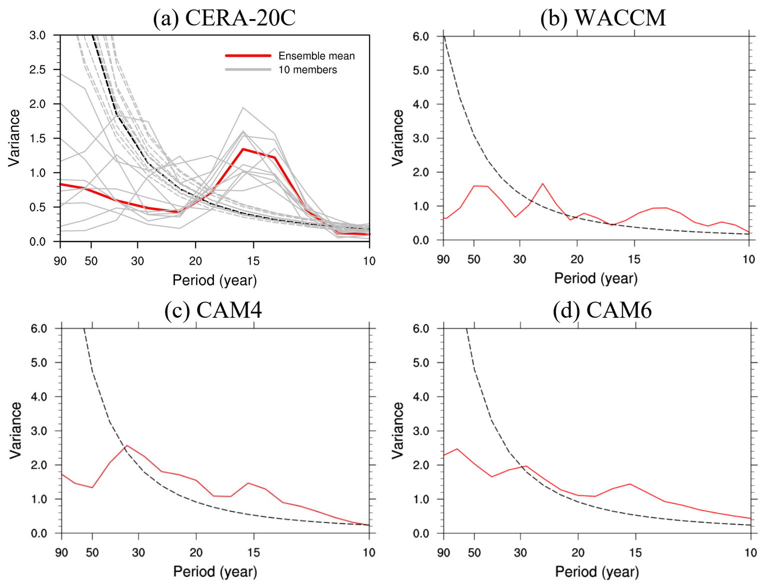

Figure 1. Power spectrum of the 10 hPa NAM index in (a) CERA-20C, (b) WACCM (high-top model), (c) CAM4 (low-top model), and (d) CAM6 (low-top model). In (a), the grey solid lines represent the power spectra from 10 individual members of CERA-20C, and the red line represents their ensemble mean. The grey dashed lines and black dashed line in (a) denote the 95% confidence levels relative to an AR(1) red-noise background for individual members and their ensemble mean, respectively. In (b-d), the red line shows the power spectrum, and the black dashed line indicates the 95% confidence level. In each model, spectra are computed from 250-year segments and then averaged.

while another peak around 10-15 years is evident in the model-year windows 50–150 and 380-470 (Figure 2b). In low-top CAM4 and CAM6 models, the wavelet spectrum displays intermittent power throughout the simulations at periods of around 15 years. A significant signal at periods of around 30 years is also evident approximately during model years 100-200 and 400-500 in CAM4 simulation (Figure 2c), and approximately during model years 1500-1800 in CAM6 simulation (Figure 2d).

Importantly, Figure 2 highlights pronounced intermittency in both the ∼15-year and 30∼40-year frequency signals across the three model simulations. Variability near 15 years is present throughout much of the integration, whereas power in the 30∼40-year band appears more episodically. Episodes of enhanced low-frequency power can persist for decades to centuries, but they weaken substantially or disappear during other periods. For example, WACCM shows little low-frequency power during model years 250-350. Moreover, the dominant frequency signal varies over time: some time intervals are characterized primarily by the ∼15-year frequency peak, some show a stronger 30∼40-year peak, and some exhibit enhanced power at both timescales. This pronounced intermittency indicates that low-frequency variability of the stratosphere is strongly non-stationary rather than exhibiting a single, persistent oscillation.

At a next step, we investigate the linkage between the stratospheric ∼15-year variability period and surface circulation using a lead-lag regression method. Because the NAM time series contains power at both ∼15 and ∼30 years, regression results can be dominated by the variability period with a larger amplitude (Dimdore-Miles et al., 2021), making it difficult to isolate the

https://doi.org/10.5194/egusphere-2026-4150
Preprint. Discussion started: 16 July 2026

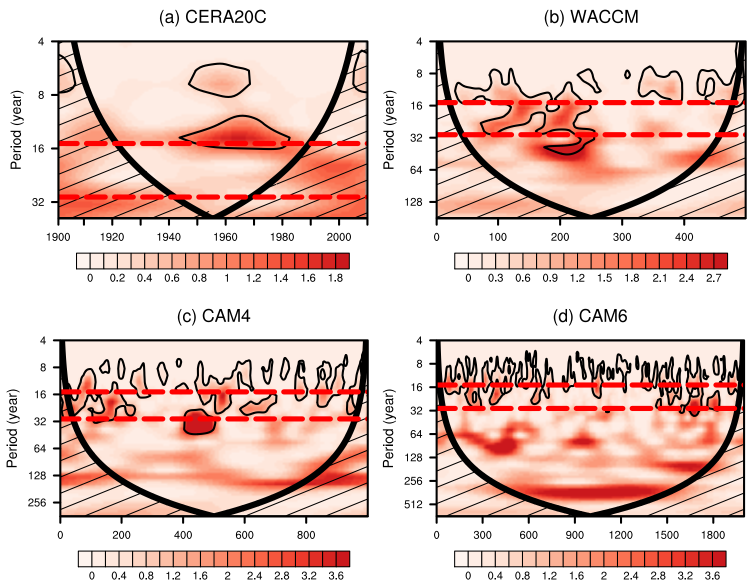

Figure 2. Wavelet power spectrum of the smoothed NAM index time series at 10 hPa in (a) CERA-20C, (b) WACCM, (c) CAM4, and (d) CAM6. Black closed contours represent the 95% confidence level, assuming a mean background AR1 red noise. The bowl-shaped thick black line indicates the cone of influence; outside this bowl, edge effects are significant and power should not be considered. Red dashed lines represent periods of ∼15 years and ∼30 years. Note the different y-axes for the different simulations due to the different simulation lengths.

surface coupling associated with each timescale. One possibility of isolating these two frequency peaks is through temporal filtering techniques, but in our case the proximity of the two peaks does not allow for a clean separation. Instead, we use the wavelet analysis (Figure 2) to identify time intervals during which the ∼15-year signal is pronounced while the ∼30-year signal is weak, and restrict the regression analysis to those intervals. Specifically, we avoid intervals where the ∼30-year peak is significant (e.g., excluding the CAM4 segment around model years 400-500, and CAM6 segment around model years 1500-1800). Accordingly, in Section 3.2 we analyze the WACCM simulation spanning the model years 10-150, the CAM4 simulation spanning the model years 500-1000, and the CAM6 simulation spanning the model years 50-1000, as indicated by the wavelet spectrum.

3.2 Link between the stratospheric ∼15-year spectral peak and surface variability

In this Section, we examine the lead-lag relationship between the stratospheric NAM index at 10 hPa and the tropospheric NAO index at the surface (Figure 3), with a focus on the stratospheric ∼15-year spectral peak identified in Figures 1 and 2. In the CERA-20C reanalysis and the model simulations, the NAM auto-regression (Figure 3, red line) exhibits a strong maximum at zero lag and secondary maxima near lags of ±15 years, consistent with the ∼15-year spectral peak observed in both the power and wavelet spectra. In CERA-20C and WACCM, the NAM auto-regression also exhibits a significant local minimum around

https://doi.org/10.5194/egusphere-2026-4150
Preprint. Discussion started: 16 July 2026

lags of ±8 years, but this feature is absent in the low-top CAM4 simulation, which is potentially related to model biases. For example, CAM4 simulates a stronger stratospheric polar vortex than observations (see discussion in Section 2 and Appendix Figure A1). In CAM6, a local minimum is present near lags of ±8 years but does not reach statistical significance.

Both reanalysis and model simulations suggest that the stratospheric ∼15-year variability period tends to lead NAO oscillation with a similar timescale. In Figure 3, positive lags indicate that the stratospheric NAM leads the tropospheric NAO, while negative lags indicate that the tropospheric NAO leads the stratospheric NAM. In CERA-20C, positive NAM anomalies are associated with positive NAO anomalies at lags near 0 and 15 years, while negative NAM anomalies are associated with negative NAO anomalies at lags near 22 years (Figure 3a). WACCM shows a similar NAM-NAO lead-lag relationship with CERA-20C reanalysis (Figure 3b), and CAM6 exhibits broadly consistent behavior at lags near 0 and 15 years (Figure 3d). By contrast, the relationship at negative lags is generally weak and not statistically significant at lags of -15 years in CERA-20C and WACCM.

Compared with CERA-20C reanalysis, WACCM and CAM6, the low-top model CAM4 shows a much weaker lead-lag relationship between the stratospheric NAM and the tropospheric NAO (Figure 3c). Specifically, the NAO signal near zero lag (blue line) is substantially weaker, and the NAO response near the 15-year lags is not evident, suggesting that CAM4 has limited skill in simulating low-frequency stratosphere–NAO coupling. The misrepresented stratosphere-troposphere coupling may further feed back to the muted signal of the stratospheric ∼15-year frequency peak. In contrast, the low-top model CAM6 broadly reproduces the ∼15-year variability period of the stratosphere and its link with the NAO. This improved performance may be related to CAM6's better representation of the wave-1 and wave-2 components of 10 hPa geopotential height (Figure A1), and CAM6's higher horizontal and vertical resolution than CAM4, which together support a more realistic representation of low-frequency stratosphere–troposphere coupling compared to CAM4.

The overall lead-lag relationship between the stratospheric ∼15-year variability period and the NAO is not sensitive to the specific choice of analysis time windows. When we repeat the analysis using alternative time intervals that predominantly feature the ∼15-year spectral peak, such as model years 500–1000 or 600-1200 in CAM6, and model years 600–900 in CAM4 (Figure A2), the results remain broadly consistent with Figure 3. CAM6 continues to show a significant positive NAO anomaly at lags near 0 and 15 years following positive NAM anomalies, whereas CAM4 shows a much weaker and generally insignificant lead-lag relationship. These sensitivity tests suggest that our main conclusions remain similar as long as the selected intervals are characterized by a significant ∼15-year peak but a non-significant ∼30-40-year peak.

For the North Pacific, Figure 4 shows the lead-lag regression between the stratospheric NAM index at 10 hPa and the tropospheric Aleutian Low index at the surface (blue line), as well as the PDO index (green line). In both CERA-20C reanalysis (Figure 4a) and WACCM (Figure 4b), positive NAM anomalies are associated with a weakened Aleutian Low and a negative PDO near zero lag. This is consistent with previous work suggesting that a weakened Aleutian Low and negative PDO can strengthen the stratospheric polar vortex by reducing upward Rossby wave propagation into the stratosphere (Garfinkel et al., 2010; Hu and Guan, 2018). However, at lags near ±15 years, CERA-20C shows a negligible Aleutian Low and PDO signal when the NAM is significantly positive. Although WACCM simulates a generally anti-correlated relationship between the Aleutian Low and the stratospheric ∼15-year spectral peak (Figure 4b, red line and blue line), the Aleutian Low anomaly is

https://doi.org/10.5194/egusphere-2026-4150
Preprint. Discussion started: 16 July 2026

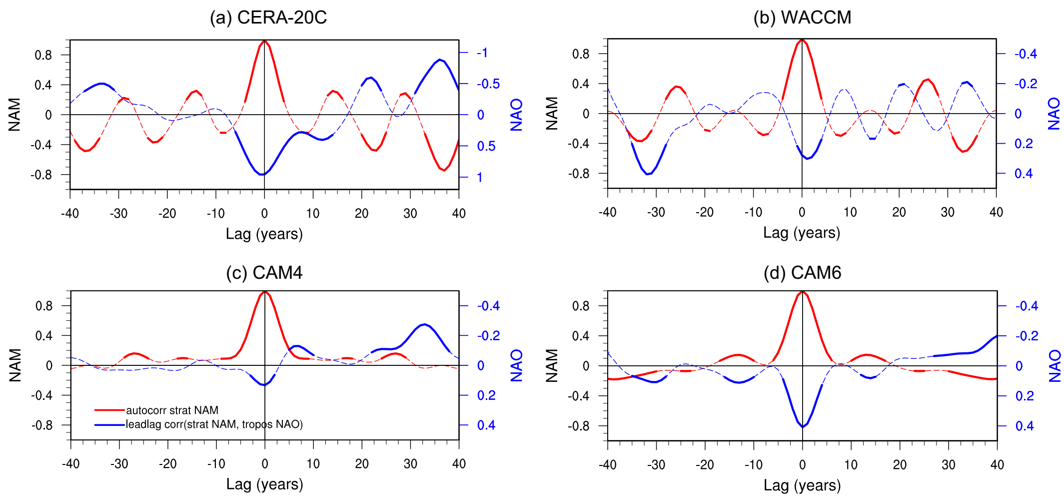

Figure 3. Lagged regression of the tropospheric NAO index (blue line) with the stratospheric NAM index. Note that the right y-axis for NAO is inverted (labels decrease upward) for display purposes. Red lines represent the auto-regression of the stratospheric NAM index. To focus on the ∼15-year frequency peak, data from (**a**) CERA20C (1900-2010), (**b**) WACCM spanning model years 10-150, (**c**) CAM4 spanning model years 500-1000, and (**d**) CAM6 spanning model years 50-1000 are analyzed. Positive lags indicate the stratospheric polar vortex leads the surface NAO. All indices are smoothed with a Gaussian filter (σ = 2 years). Solid segments of the lines indicate regression coefficients significant at the 95% confidence level based on a Student's t-test.

only significant at lags around -18, -12, 2 and 25 years. Overall, the lead-lag relationships between stratospheric ∼15-year frequency peak and Pacific surface indices are not as clear as those found for the NAO (Figure 3). One potential explanation is that the downward coupling over the Atlantic region is stronger than that over the Pacific. It is also possible that the CERA-20C and the selected WACCM simulation are still too short to adequately capture the low-frequency linkage between the Aleutian Low and the stratospheric polar vortex. Similar to WACCM, CAM6 shows a generally anti-correlated NAM-Aleutian Low relationship during negative lags (Figure 4d), but the Aleutian Low response is weak near the positive lags around 15 years. By contrast, neither CAM6 nor CAM4 exhibits a clear relationship between the PDO and the stratospheric ∼15-year variability period, with regression coefficients close to zero near zero lag (Figures 4c,d). Taken together, the lack of agreement between CERA-20C and the model simulations suggests that the link between the stratospheric ∼15-year variability period and the Pacific circulation (the Aleutian Low and PDO) is relatively weak and less coherent than the corresponding stratosphere-NAO relationship.

To further assess the surface signatures associated with the stratospheric ∼15-year spectral peak highlighted in Figures 3 and 4, we analyze the lagged regression patterns of sea level pressure (SLP) and SST with the stratospheric NAM index (Figures 5 and A3). Results from CAM4 are not shown here due to CAM4's limited performance in simulating the stratospheric ∼15-year spectral peak and the coupling with the tropospheric circulation. Figure 5 shows the SLP regression pattern at three lags corresponding to Figure 3: a lag of -15 years (averaged over -17 to -13 years), zero lag (averaged over -2 to +2 years), and

https://doi.org/10.5194/egusphere-2026-4150
Preprint. Discussion started: 16 July 2026

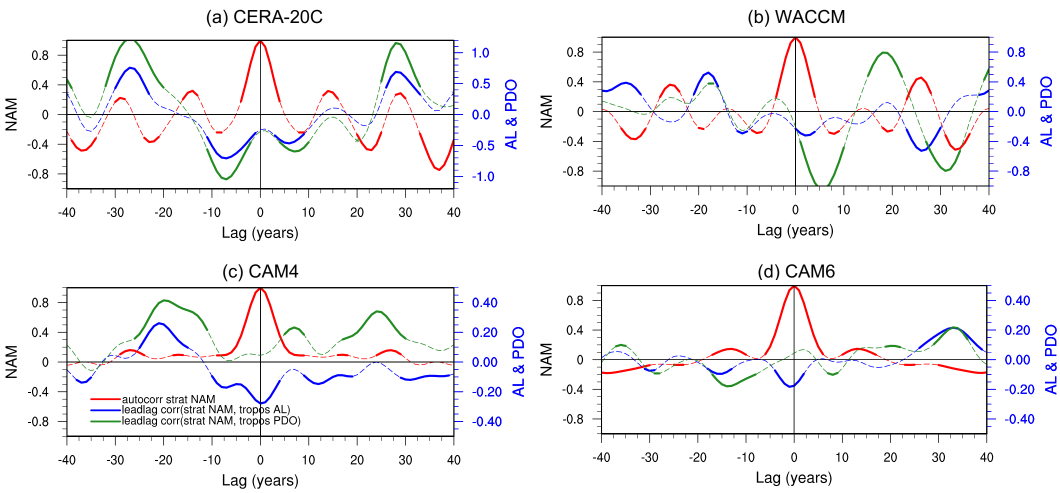

Figure 4. Lagged regression of the tropospheric Aleutian Low index (blue line) and the PDO index (green line) with the stratospheric NAM index, where positive (negative) values indicate the strong (weak) Aleutian Low anomalies. For green lines, positive (negative) values represents positive (negative) PDO anomalies. Red lines represent the auto-regression of the NAM index. To focus on the ∼15-year frequency peak, data from (**a**) CERA20C, (**b**) WACCM spanning years 10-150 of the model simulation, (**c**) CAM4 spanning years 500-1000, and (**d**) CAM6 spanning years 50-1000 are analyzed. Positive lags indicate the stratospheric polar vortex leads the Aleutian Low and PDO. All indices are smoothed with a Gaussian filter (σ = 2 years). Solid segments of the lines indicate regression coefficients significant at the 95% confidence level based on a Student's t-test.

a lag of +15 years (averaged over +13 to +17 years). In CERA-20C, WACCM, and CAM6, the dipole structure of Atlantic SLP anomalies projects onto the positive phase of the NAO at approximately zero lag and 15-year lag during positive NAM anomalies, whereas the NAO-like signal is weak and not significant at -15 years in CERA-20C and WACCM. These spatial patterns corroborate the lead–lag regression results in Figure 3, indicating that stratospheric variability in the ∼15-year period is closely associated with an NAO-like surface circulation and tends to lead NAO variability on a comparable timescale. Both WACCM and CAM6 to some extent capture the lagged NAO-like SLP response near lags of 15 years observed in CERA-20C reanalysis, although the North Atlantic SLP anomalies in CAM6 are weaker. In CERA-20C, the SST regression patterns (Figure A3a) display a tripole structure over the North Atlantic around zero and 15-year lags, with positive anomalies over the subpolar North Atlantic between approximately 50–65° N, negative anomalies off the East Coast of North America, and a second positive anomaly off the coast of northeast Africa. This SST tripole pattern aligns with the SST pattern associated with a positive NAO (Delworth and Zeng, 2016) and may provide a pathway through which the atmosphere can influence longer-term ocean variability (e.g., the Atlantic meridional overturning circulation). Compared with CERA-20C, WACCM reproduces a similar tripole pattern at lags near 0 and +15 years, while CAM6 captures a comparable structure at zero lag but exhibits a different SST pattern at +15 years.

https://doi.org/10.5194/egusphere-2026-4150
Preprint. Discussion started: 16 July 2026

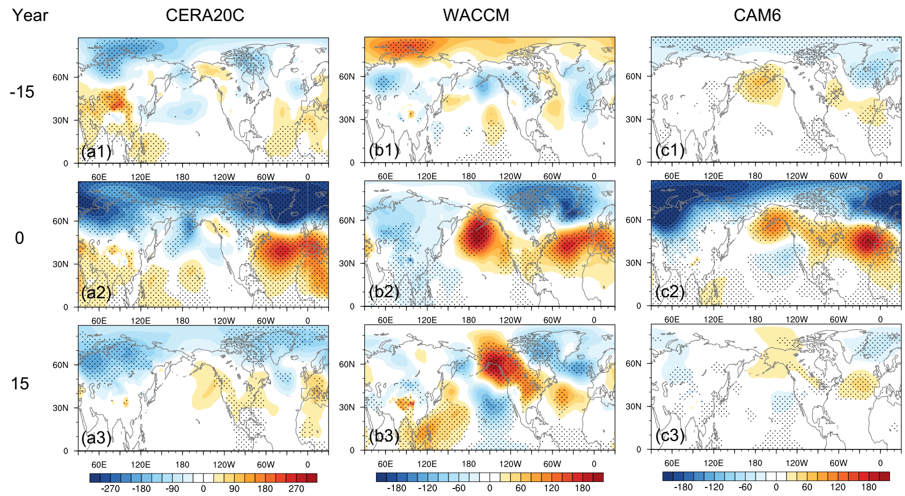

Figure 5. Lagged regression patterns of sea level pressure (SLP) with the stratospheric NAM index for (**a**) CERA-20C, (**b**) WACCM (model years 10-150), (**c**) CAM6 (model years 50-1000). From top to bottom, the panels show the regression patterns at -15-year lag (averaged over years -13∼-17), zero lag (averaged over years -2∼2), and 15-year lag (averaged over years 13∼17). Positive lags indicate that the stratospheric polar vortex precedes the surface circulation. Stippling indicates the regression coefficients significant at the 95% confidence level based on a Student's *t*-test.

Over the North Pacific, the lagged SLP and SST patterns in WACCM and CAM6 do not match those in CERA-20C. For example, CERA-20C shows negative SLP anomalies around the Bering Strait region around zero lag, whereas the WACCM and CAM6 display positive anomalies. Additionally, the SLP and SST anomalies over the North Pacific are generally weak and not statistically significant near lags of -15 and +15 years in CERA-20C, consistent with the comparatively weak and less coherent lead–lag relationships between the stratospheric ∼15-year variability and Pacific indices (Aleutian Low and PDO) inferred from Figure 4. Considering the inconsistency between models and reanalysis, the relationship between the stratospheric ∼15-year frequency peak and North Pacific surface circulation remains uncertain and warrants further evaluation using additional high-top models and longer observational record.

3.3 Stratospheric ∼30-40 year spectral peaks

In addition to the dominant ∼15-year spectral peak, CESM simulations exhibit a lower-frequency peak around ∼30-40 years (Figures 1 and 2). In WACCM, a pronounced ∼30-40-year peak emerges around model years 150–250, while CAM4 and CAM6 display episodic ∼30-year peaks around model years 400–500 and 1500–1800, respectively. A similar multi-decadal stratospheric spectral peak has been found in a 1000-year high-top UKESM simulation (Figure 7 in Dimdore-Miles et al. (2022)), where stratospheric variability near 30 years was found to precede NAO and AMOC oscillations of comparable periods. To explore the potential link with the troposphere, we select the WACCM simulation spanning model years 150-250, CAM4 spanning years 50-500, and CAM6 spanning years 1500-2000, during which the stratospheric ∼30-40-year frequency

https://doi.org/10.5194/egusphere-2026-4150
Preprint. Discussion started: 16 July 2026

peak signal is pronounced and clearly evident in the wavelet analysis (Figure 2). During these time intervals, WACCM and CAM6 simulations suggest that the stratospheric ∼30-40-year frequency peak is associated with the tropospheric NAO (blue line versus red line in Figure 6a, c), which is in agreement with the findings in Dimdore-Miles et al. (2022). In contrast, the potential relationship between the stratospheric ∼30-40-year frequency peak and the NAO is not simulated in CAM4 due to the negligible regression coefficient near zero lag. Over the North Pacific, the WACCM simulation suggests a possible association between the stratospheric ∼30-40-year frequency peak and the Aleutian Low and the PDO, primarily during negative lags (blue line versus red line in Figure 6d, f). A weak Aleutian Low and negative PDO anomalies are associated with a persistently strong polar vortex near zero lag, and a strong Aleutian Low and positive PDO anomalies are associated with a persistently weak polar vortex near lags of around -20 years. The regression coefficients linking the stratospheric ∼30-40-year spectral peak to the Aleutian Low are much weaker in CAM4 and CAM6 than in WACCM. Consistent with this, CAM4 and CAM6 show an unclear relationship between the stratospheric ∼30-40-year peak and the PDO (green lines in Figure 6e, f).

However, the results related to the stratospheric ∼30-40-year spectral peak should be interpreted with caution. This peak is identified only in the model simulations and is not evident in the reanalysis, raising the possibility that it reflects model-specific variability rather than a robust feature in observations. Our assessment is likely affected by model biases and limited effective sample sizes at multi-decadal timescales. In the high-top WACCM simulation, only a relatively short time interval (∼100 years) is available to examine the ∼30-40-year frequency peak. In addition, the low-top models CAM4 and CAM6 have comparatively coarse vertical resolution in the stratosphere and exhibit biases in the simulated stratospheric polar vortex (Figure A1), which may affect stratospheric multi-decadal variability and its coupling to the troposphere. Therefore, in this study, we simply document the possible signatures of the stratospheric ∼30-40-year frequency peak in current CESM long-term simulations.

4 Discussion and Conclusions

In this study, we investigate multi-year to multi-decadal variability of the stratospheric polar vortex and its links to the tropospheric circulation over the North Atlantic and North Pacific using the ECMWF CERA-20C reanalysis (1900–2010) and three multi-century CESM simulations: CESM1.0-CAM4 integrated for 1000 years, CESM2.0-WACCM integrated for 500 years and CESM2.0-CAM6 integrated for 2000 years. Across CERA-20C and all three model simulations, the smoothed stratospheric NAM index exhibits a prominent variability timescale near 15 years (Figure 1 and Figure 2). Wavelet analysis further shows that stratospheric low-frequency variability is highly non-stationary and intermittent, owing to the coexistence of variability at longer timescales, including episodic ∼30-40-year signals in the model simulations that are not present in the reanalysis. Accordingly, the relative prominence of the ∼15-year and longer-period peaks varies substantially over time, and in some intervals no clear low-frequency spectral peak is evident, indicating that the stratospheric low-frequency variability does not behave as a persistent single-frequency oscillation. Lead–lag regression and lagged surface patterns indicate that this stratospheric ∼15-year variability period is closely associated with NAO-like SLP anomalies and tends to lead an oscillatory NAO response on a comparable timescale (Figure 3 and Figure 5). By contrast, the corresponding relationships with North

https://doi.org/10.5194/egusphere-2026-4150
Preprint. Discussion started: 16 July 2026

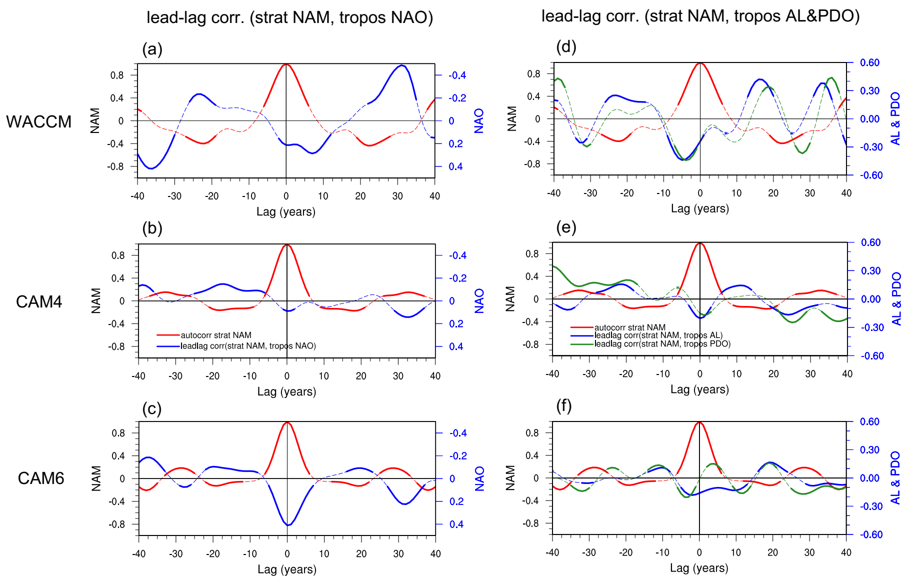

Figure 6. As in Figure 3 and Figure 4, but selecting different time intervals to focus on the stratospheric ∼30-40-year frequency peak, with (**a, b**) WACCM spanning years 150-250 of the model simulation, (**c, d**) CAM4 spanning years 50-500, and (**e, f**) CAM6 spanning years 1500-2000. Positive lags indicate that the stratospheric polar vortex leads surface circulation indices. All indices are smoothed with a Gaussian filter ($\sigma = 2$ years). Solid segments of the lines indicate regression coefficients significant at the 95% confidence level based on a Student's *t*-test.

Pacific variability are comparatively weak and less consistent between the reanalysis and model simulations (Figure 4 and Figure 5), suggesting that the Pacific linkage to the stratospheric ∼15-year variability period is more uncertain than the Atlantic linkage.

The models display both agreement and model dependence in representing the link between stratospheric ∼15-year variability period and tropospheric circulation. Consistent with CERA-20C reanalysis, the high-top model WACCM and the low-top model CAM6 reproduce the ∼15-year stratospheric spectral peak and its lead–lag relationship with the NAO. In contrast, CAM4 exhibits a much weaker lead–lag relationship between the stratospheric NAM and the tropospheric NAO and a muted expression of the ∼15-year spectral peak, indicating limited skill in simulating low-frequency stratospheric variability and its surface coupling. Although CAM6 shows some discrepancies in the North Atlantic SST response compared with CERA-20C and WACCM, it represents the stratosphere–NAO coupling far more realistically than CAM4. This improvement may be related to CAM6's higher horizontal and vertical resolution, but the specific processes responsible for CAM6's superior performance remain to be clarified.

This study helps improve our understanding of low-frequency stratospheric variability and its surface impacts. Building on previous studies showing that low-frequency variability of the stratospheric polar vortex tends to lead an oscillatory response of the tropospheric NAO (Reichler et al., 2012; Dimdore-Miles et al., 2022), we further show that this low-frequency strato-

https://doi.org/10.5194/egusphere-2026-4150
Preprint. Discussion started: 16 July 2026

sphere–NAO coupling also occurs at a ∼15-year timescale by comparing the CERA-20C reanalysis with multiple long CESM simulations. Lead–lag regression patterns further indicate that stratospheric ∼15-year variability has a downward influence on SLP and SST variability over the North Atlantic at a similar timescale, thereby potentially shaping the climate over the Northern Hemisphere middle-to-high latitudes. A better understanding of the mechanisms underlying low-frequency stratosphere–troposphere coupling may therefore help improve decadal climate prediction. More broadly, these findings highlight the importance of accurately representing the stratosphere in climate models.

The conclusions drawn in this study could be affected by the length of the reanalysis record and model biases. The available reanalysis record is likely not long enough to accurately capture low-frequency stratospheric variability. Analysis of long-term model simulations remains the only available method for understanding this problem. However, strong model deficiencies and biases need to be kept in mind. Previous studies have found that different vertical resolution and dynamical cores in general circulation models can substantially impact the simulation of SSW occurrence (Yao and Jablonowski, 2016; Chávez et al., 2022). For example, due to low vertical resolutions, CESM2.0-CAM6 simulates a lower frequency of split, displacement and mixed SSW events than observations (Wu and Reichler, 2020; Hall et al., 2021). Although CESM2.0-WACCM has high vertical resolution, it underestimates the SSW frequency compared with ERA5 (Hall et al., 2021). Regarding low-frequency coupling between the stratosphere and the troposphere, Reichler et al. (2012) demonstrated that the North Atlantic surface response to persistent SSW events is significantly weaker in CMIP5 low-top models, including CESM1.0-CAM4, compared to high-top models. Therefore, studies using a longer reanalysis record and long-term high-top model simulations are required for a better understanding of low-frequency stratospheric variability and its coupling to the troposphere.

Appendix A: Supplementary figures

https://doi.org/10.5194/egusphere-2026-4150
Preprint. Discussion started: 16 July 2026

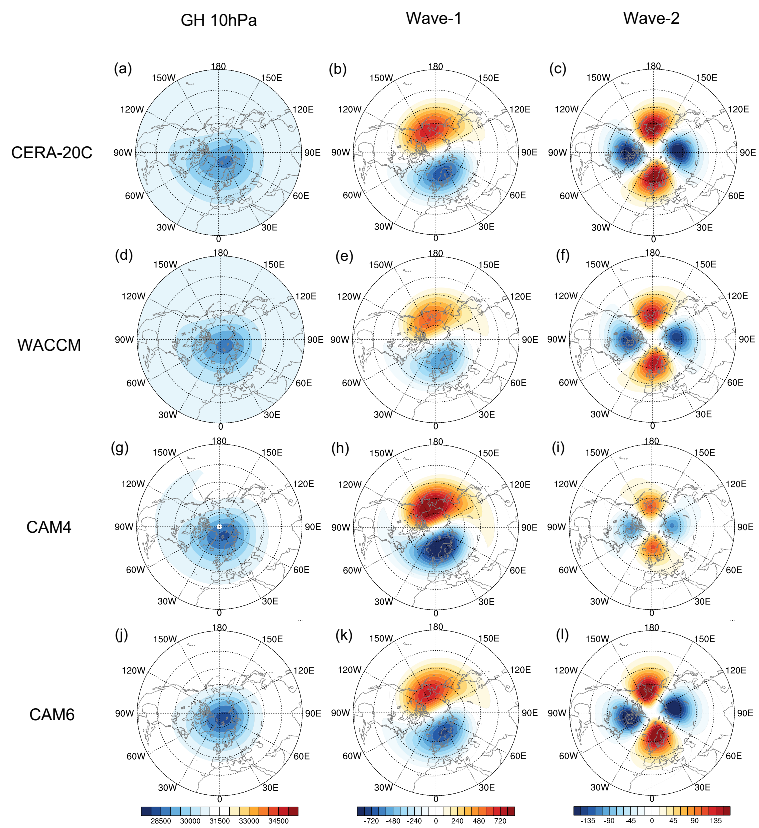

Figure A1. Comparison of model representations of climatological 10 hPa geopotential height (left panels; units: m), and its wave-1 (middle panels) and wave-2 (right panels) components, with CERA-20C reanalysis. The wave-1 and wave-2 components are obtained from a Fourier decomposition of the climatological 10 hPa geopotential height. (a-c) CERA-20C reanalysis averaged over 1900-2010; (d-f) WACCM (high-top model) averaged over 500 simulation years; (g-i) CAM4 (low-top model) averaged over 1000 simulation years, and (j-l) CAM6 (low-top model) averaged over 2000 simulation years. All variables are averaged over November-March

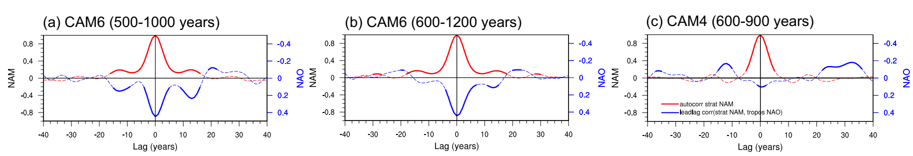

Figure A2. Same as Figure 3, but for different model time intervals. (a) and (b) show CAM6 averaged over model years 500–1000 and 600–1200, respectively, and (c) shows CAM4 averaged over model years 600–900.

https://doi.org/10.5194/egusphere-2026-4150
Preprint. Discussion started: 16 July 2026

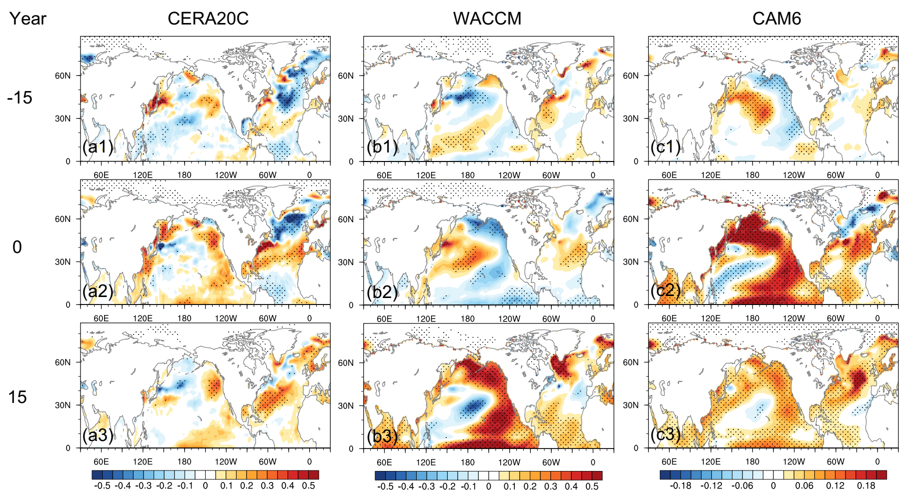

Figure A3. Similar to Figure 5, but for the lagged regression patterns of sea surface temperature (SST) with the stratospheric NAM index.

https://doi.org/10.5194/egusphere-2026-4150
Preprint. Discussion started: 16 July 2026

Data availability. The data used in this study are freely and publicly available. The CERA-20C reanalysis is available from the ECMWF Public Datasets archive (https://apps.ecmwf.int/datasets/; Laloyaux et al. (2018)). The CESM2-CAM6 and CESM2-WACCM piControl simulations are available from the CMIP6 archive via the Earth System Grid Federation (ESGF; https://esgf-node.llnl.gov/search/cmip6/; Danabasoglu et al. (2020). The CESM1.0-CAM4 simulation data used in this study are available at Zenodo (https://doi.org/10.5281/zenodo.21268962).

Author contributions. LW, DD, and GC designed the study. LW performed the analysis and wrote the original manuscript. All authors contributed to the interpretation of the results and edited the manuscript.

Competing interests. D.D. is a member of the editorial board of Weather and Climate Dynamics. The authors have no other competing interests to declare.

Acknowledgements. We thank Kevin M. Grise at University of Virginia for helpful discussions on an earlier version of the manuscript. We also thank Andries de Vries at University of Lausanne for help with access to CERA-20C, and Lantao Sun at Colorado State University for help with access to the WACCM and CAM6 simulations at NCAR. D.D. acknowledges support from the Swiss National Science Foundation through project PP00P2_198896. G.C. is supported by NSF Grant AGS-2232581. H.Y. acknowledges support from the National Science Foundation of China (Nos., 41725021, 42230403, 42288101).

References

Ayarzagüena, B., Manzini, E., Calvo, N., and Matei, D.: Interaction between decadal-to-multidecadal oceanic variability and sudden stratospheric warmings, Annals of the New York Academy of Sciences, 1504, 215–229, https://doi.org/10.1111/nyas.14663, 2021.

Baldwin, M. P. and Dunkerton, T. J.: Stratospheric Harbingers of Anomalous Weather Regimes, Science, 294, 581–584, https://doi.org/10.1126/science.1063315, 2001.

Baldwin, M. P., Ayarzagüena, B., Birner, T., Butchart, N., Butler, A. H., Charlton-Perez, A. J., Domeisen, D. I. V., Garfinkel, C. I., Garny, H., Gerber, E. P., Hegglin, M. I., Langematz, U., and Pedatella, N. M.: Sudden Stratospheric Warmings, Reviews of Geophysics, 59, e2020RG000 708, https://doi.org/10.1029/2020RG000708, 2021.

Bett, P. E., Scaife, A. A., Hardiman, S. C., Thornton, H. E., Shen, X., Wang, L., and Pang, B.: Using large ensembles to quantify the impact of sudden stratospheric warmings and their precursors on the North Atlantic Oscillation, Weather and Climate Dynamics, 4, 213–228, https://doi.org/10.5194/wcd-4-213-2023, 2023.

Butler, A. H., Seidel, D. J., Hardiman, S. C., Butchart, N., Birner, T., and Match, A.: Defining Sudden Stratospheric Warmings, Bulletin of the American Meteorological Society, 96, 1913–1928, https://doi.org/10.1175/BAMS-D-13-00173.1, 2015.

Butler, A. H., Karpechko, A. Y., and Garfinkel, C. I.: Amplified Decadal Variability of Extratropical Surface Temperatures by Stratosphere-Troposphere Coupling, Geophysical Research Letters, 50, e2023GL104 607, https://doi.org/10.1029/2023GL104607, 2023.

Charlton, A. J. and Polvani, L. M.: A New Look at Stratospheric Sudden Warmings. Part I: Climatology and Modeling Benchmarks, Journal of Climate, 20, 449–469, https://doi.org/10.1175/JCLI3996.1, 2007.

Chen, G. and Ding, X.: Benchmarking the Dynamic Modes of Stratosphere-Troposphere Coupling in Northern Annular Modes (NAM) in CMIP6 Models, Geophysical Research Letters, 53, e2025GL121 278, https://doi.org/10.1029/2025GL121278, 2026.

Chávez, V. M., Añel, J. A., Garcia, R. R., Šácha, P., and Torre, L. d. l.: Impact of Increased Vertical Resolution in WACCM on the Climatology of Major Sudden Stratospheric Warmings, Atmosphere, 13, 546, https://doi.org/10.3390/atmos13040546, 2022.

Coulibaly, P. and Burn, D. H.: Wavelet analysis of variability in annual Canadian streamflows, Water Resources Research, 40, 2003WR002 667, https://doi.org/10.1029/2003WR002667, 2004.

Danabasoglu, G., Lamarque, J., Bacmeister, J., Bailey, D. A., DuVivier, A. K., Edwards, J., Emmons, L. K., Fasullo, J., Garcia, R., Gettelman, A., Hannay, C., Holland, M. M., Large, W. G., Lauritzen, P. H., Lawrence, D. M., Lenaerts, J. T. M., Lindsay, K., Lipscomb, W. H., Mills, M. J., Neale, R., Oleson, K. W., Otto-Bliesner, B., Phillips, A. S., Sacks, W., Tilmes, S., Van Kampenhout, L., Vertenstein, M., Bertini, A., Dennis, J., Deser, C., Fischer, C., Fox-Kemper, B., Kay, J. E., Kinnison, D., Kushner, P. J., Larson, V. E., Long, M. C., Mickelson, S., Moore, J. K., Nienhouse, E., Polvani, L., Rasch, P. J., and Strand, W. G.: The Community Earth System Model Version 2 (CESM2), Journal of Advances in Modeling Earth Systems, 12, e2019MS001 916, https://doi.org/10.1029/2019MS001916, 2020.

Delworth, T. L. and Zeng, F.: The Impact of the North Atlantic Oscillation on Climate through Its Influence on the Atlantic Meridional Overturning Circulation, Journal of Climate, 29, 941–962, https://doi.org/10.1175/JCLI-D-15-0396.1, 2016.

Dimdore-Miles, O., Gray, L., and Osprey, S.: Origins of multi-decadal variability in sudden stratospheric warmings, Weather and Climate Dynamics, 2, 205–231, https://doi.org/10.5194/wcd-2-205-2021, 2021.

Dimdore-Miles, O., Gray, L., Osprey, S., Robson, J., Sutton, R., and Sinha, B.: Interactions between the stratospheric polar vortex and Atlantic circulation on seasonal to multi-decadal timescales, Atmospheric Chemistry and Physics, 22, 4867–4893, https://doi.org/10.5194/acp-22-4867-2022, 2022.

Ding, X., Chen, G., Sun, L., and Zhang, P.: Distinct North American Cooling Signatures Following the Zonally Symmetric and Asymmetric Modes of Winter Stratospheric Variability, Geophysical Research Letters, 49, e2021GL096 076, https://doi.org/10.1029/2021GL096076, 2022.

Ding, X., Chen, G., Zhang, P., Domeisen, D. I. V., and Orbe, C.: Extreme stratospheric wave activity as harbingers of cold events over North America, Communications Earth & Environment, 4, 187, https://doi.org/10.1038/s43247-023-00845-y, 2023.

Domeisen, D. I. V.: Estimating the Frequency of Sudden Stratospheric Warming Events From Surface Observations of the North Atlantic Oscillation, Journal of Geophysical Research: Atmospheres, 124, 3180–3194, https://doi.org/10.1029/2018JD030077, 2019.

Domeisen, D. I. V. and Butler, A. H.: Stratospheric drivers of extreme events at the Earth's surface, Communications Earth & Environment, 1, 1–8, https://doi.org/10.1038/s43247-020-00060-z, 2020.

Domeisen, D. I. V., Badin, G., and Koszalka, I. M.: How Predictable Are the Arctic and North Atlantic Oscillations? Exploring the Variability and Predictability of the Northern Hemisphere, Journal of Climate, 31, 997–1014, https://doi.org/10.1175/JCLI-D-17-0226.1, 2018.

Domeisen, D. I. V., Garfinkel, C. I., and Butler, A. H.: The Teleconnection of El Niño Southern Oscillation to the Stratosphere, Reviews of Geophysics, 57, 5–47, https://doi.org/10.1029/2018RG000596, 2019.

Domeisen, D. I. V., Butler, A. H., Charlton-Perez, A. J., Ayarzagüena, B., Baldwin, M. P., Dunn-Sigouin, E., Furtado, J. C., Garfinkel, C. I., Hitchcock, P., Karpechko, A. Y., Kim, H., Knight, J., Lang, A. L., Lim, E., Marshall, A., Roff, G., Schwartz, C., Simpson, I. R., Son, S., and Taguchi, M.: The Role of the Stratosphere in Subseasonal to Seasonal Prediction: 2. Predictability Arising From Stratosphere-Troposphere Coupling, Journal of Geophysical Research: Atmospheres, 125, e2019JD030 923, https://doi.org/10.1029/2019JD030923, 2020.

Feldstein, S. B. and Franzke, C.: Are the North Atlantic Oscillation and the Northern Annular Mode Distinguishable?, Journal of the Atmospheric Sciences, 63, 2915–2930, https://doi.org/10.1175/JAS3798.1, 2006.

Garfinkel, C. I., Hartmann, D. L., and Sassi, F.: Tropospheric Precursors of Anomalous Northern Hemisphere Stratospheric Polar Vortices, Journal of Climate, 23, 3282–3299, https://doi.org/10.1175/2010JCLI3010.1, 2010.

Gettelman, A., Mills, M. J., Kinnison, D. E., Garcia, R. R., Smith, A. K., Marsh, D. R., Tilmes, S., Vitt, F., Bardeen, C. G., McInerny, J., Liu, H., Solomon, S. C., Polvani, L. M., Emmons, L. K., Lamarque, J., Richter, J. H., Glanville, A. S., Bacmeister, J. T., Phillips, A. S., Neale, R. B., Simpson, I. R., DuVivier, A. K., Hodzic, A., and Randel, W. J.: The Whole Atmosphere Community Climate Model Version 6 (WACCM6), Journal of Geophysical Research: Atmospheres, 124, 12 380–12 403, https://doi.org/10.1029/2019JD030943, 2019.

Grinsted, A., Moore, J. C., and Jevrejeva, S.: Application of the cross wavelet transform and wavelet coherence to geophysical time series, Nonlinear Processes in Geophysics, 11, 561–566, https://doi.org/10.5194/npg-11-561-2004, 2004.

Hall, R. J., Mitchell, D. M., Seviour, W. J. M., and Wright, C. J.: Persistent Model Biases in the CMIP6 Representation of Stratospheric Polar Vortex Variability, Journal of Geophysical Research: Atmospheres, 126, e2021JD034 759, https://doi.org/10.1029/2021JD034759, 2021.

Hu, D. and Guan, Z.: Decadal Relationship between the Stratospheric Arctic Vortex and Pacific Decadal Oscillation, Journal of Climate, 31, 3371–3386, https://doi.org/10.1175/JCLI-D-17-0266.1, 2018.

Hurrell, J. W., Kushnir, Y., and Visbeck, M.: The North Atlantic Oscillation, Science, 291, 603–605, https://doi.org/10.1126/science.1058761, 2001.

Karpechko, A. Y., Afargan-Gerstman, H., Butler, A. H., Domeisen, D. I. V., Kretschmer, M., Lawrence, Z., Manzini, E., Sigmond, M., Simpson, I. R., and Wu, Z.: Northern Hemisphere Stratosphere-Troposphere Circulation Change in CMIP6 Models: 1. Inter-Model Spread and Scenario Sensitivity, Journal of Geophysical Research: Atmospheres, 127, e2022JD036 992, https://doi.org/10.1029/2022JD036992, 2022.

https://doi.org/10.5194/egusphere-2026-4150
Preprint. Discussion started: 16 July 2026

Kidston, J., Scaife, A. A., Hardiman, S. C., Mitchell, D. M., Butchart, N., Baldwin, M. P., and Gray, L. J.: Stratospheric influence on tropospheric jet streams, storm tracks and surface weather, Nature Geoscience, 8, 433–440, https://doi.org/10.1038/ngeo2424, 2015.

Kodera, K. and Kuroda, Y.: Dynamical response to the solar cycle, Journal of Geophysical Research: Atmospheres, 107, https://doi.org/10.1029/2002JD002224, 2002.

Kren, A. C., Marsh, D. R., Smith, A. K., and Pilewskie, P.: Wintertime Northern Hemisphere Response in the Stratosphere to the Pacific Decadal Oscillation Using the Whole Atmosphere Community Climate Model, Journal of Climate, 29, 1031–1049, https://doi.org/10.1175/JCLI-D-15-0176.1, 2016.

Laloyaux, P., De Boisseson, E., Balmaseda, M., Bidlot, J., Broennimann, S., Buizza, R., Dalhgren, P., Dee, D., Haimberger, L., Hersbach, H., Kosaka, Y., Martin, M., Poli, P., Rayner, N., Rustemeier, E., and Schepers, D.: CERA-20C: A Coupled Reanalysis of the Twentieth Century, Journal of Advances in Modeling Earth Systems, 10, 1172–1195, https://doi.org/10.1029/2018MS001273, 2018.

Li, Y., Tian, W., Xie, F., Wen, Z., Zhang, J., Hu, D., and Han, Y.: The connection between the second leading mode of the winter North Pacific sea surface temperature anomalies and stratospheric sudden warming events, Climate Dynamics, 51, 581–595, https://doi.org/10.1007/s00382-017-3942-0, 2018.

Linkin, M. E. and Nigam, S.: The North Pacific Oscillation–West Pacific Teleconnection Pattern: Mature-Phase Structure and Winter Impacts, Journal of Climate, 21, 1979–1997, https://doi.org/10.1175/2007JCLI2048.1, 2008.

Lorenzo, E. D., Xu, T., Zhao, Y., Newman, M., Capotondi, A., Stevenson, S., Amaya, D. J., Anderson, B. T., Ding, R., Furtado, J. C., Joh, Y., Liguori, G., Lou, J., Miller, A. J., Navarra, G., Schneider, N., Vimont, D. J., Wu, S., and Zhang, H.: Modes and Mechanisms of Pacific Decadal-Scale Variability, Annual Review of Marine Science, 15, 249–275, https://doi.org/10.1146/annurev-marine-040422-084555, 2023.

Manney, G. L., Krüger, K., Sabutis, J. L., Sena, S. A., and Pawson, S.: The remarkable 2003–2004 winter and other recent warm winters in the Arctic stratosphere since the late 1990s, Journal of Geophysical Research: Atmospheres, 110, 2004JD005 367, https://doi.org/10.1029/2004JD005367, 2005.

Mantua, N. J., Hare, S. R., Zhang, Y., Wallace, J. M., and Francis, R. C.: A Pacific Interdecadal Climate Oscillation with Impacts on Salmon Production*, Bulletin of the American Meteorological Society, 78, 1069–1080, https://doi.org/10.1175/1520-0477(1997)078<1069:APICOW>2.0.CO;2, 1997.

Manzini, E., Cagnazzo, C., Fogli, P. G., Bellucci, A., and Müller, W. A.: Stratosphere-troposphere coupling at inter-decadal time scales: Implications for the North Atlantic Ocean, Geophysical Research Letters, 39, https://doi.org/10.1029/2011GL050771, _eprint: https://onlinelibrary.wiley.com/doi/pdf/10.1029/2011GL050771, 2012.

Nalley, D., Adamowski, J., Biswas, A., Gharabaghi, B., and Hu, W.: A multiscale and multivariate analysis of precipitation and streamflow variability in relation to ENSO, NAO and PDO, Journal of Hydrology, 574, 288–307, https://doi.org/10.1016/j.jhydrol.2019.04.024, 2019.

Omrani, N.-E., Keenlyside, N. S., Bader, J., and Manzini, E.: Stratosphere key for wintertime atmospheric response to warm Atlantic decadal conditions, Climate Dynamics, 42, 649–663, https://doi.org/10.1007/s00382-013-1860-3, 2014.

Omrani, N.-E., Keenlyside, N., Matthes, K., Boljka, L., Zanchettin, D., Jungclaus, J. H., and Lubis, S. W.: Coupled stratosphere-troposphere-Atlantic multidecadal oscillation and its importance for near-future climate projection, npj Climate and Atmospheric Science, 5, 59, https://doi.org/10.1038/s41612-022-00275-1, 2022.

Pawson, S. and Naujokat, B.: The cold winters of the middle 1990s in the northern lower stratosphere, Journal of Geophysical Research: Atmospheres, 104, 14 209–14 222, https://doi.org/10.1029/1999JD900211, 1999.

https://doi.org/10.5194/egusphere-2026-4150
Preprint. Discussion started: 16 July 2026

Reichler, T., Kim, J., Manzini, E., and Kröger, J.: A stratospheric connection to Atlantic climate variability, Nature Geoscience, 5, 783–787, https://doi.org/10.1038/ngeo1586, 2012.

Schimanke, S., Körper, J., Spangehl, T., and Cubasch, U.: Multi-decadal variability of sudden stratospheric warmings in an AOGCM: LONGTERM VARIABILITY OF SSWS, Geophysical Research Letters, 38, n/a–n/a, https://doi.org/10.1029/2010GL045756, 2011.

Seviour, W. J. M.: Weakening and shift of the Arctic stratospheric polar vortex: Internal variability or forced response?, Geophysical Research Letters, 44, 3365–3373, https://doi.org/10.1002/2017GL073071, 2017.

Shen, X., Wang, L., Scaife, A. A., Hardiman, S. C., and Xu, P.: The Stratosphere–Troposphere Oscillation as the Dominant Intraseasonal Coupling Mode between the Stratosphere and Troposphere, Journal of Climate, 36, 2259–2276, https://doi.org/10.1175/JCLI-D-22-0238.1, 2023.

Simpson, I. R., Hitchcock, P., Seager, R., Wu, Y., and Callaghan, P.: The Downward Influence of Uncertainty in the Northern Hemisphere Stratospheric Polar Vortex Response to Climate Change, Journal of Climate, 31, 6371–6391, https://doi.org/10.1175/JCLI-D-18-0041.1, 2018.

Thompson, D. W. J. and Wallace, J. M.: Regional Climate Impacts of the Northern Hemisphere Annular Mode, Science, 293, 85–89, https://doi.org/10.1126/science.1058958, 2001.

Torrence, C. and Compo, G. P.: A Practical Guide to Wavelet Analysis, Bulletin of the American Meteorological Society, 79, 61–78, https://doi.org/10.1175/1520-0477(1998)079<0061:APGTWA>2.0.CO;2, 1998.

Wang, L. and Chen, W.: Downward Arctic Oscillation signal associated with moderate weak stratospheric polar vortex and the cold December 2009, Geophysical Research Letters, 37, 2010GL042 659, https://doi.org/10.1029/2010GL042659, 2010.

Whitcher, B., Guttorp, P., and Percival, D. B.: Wavelet analysis of covariance with application to atmospheric time series, Journal of Geophysical Research: Atmospheres, 105, 14 941–14 962, https://doi.org/10.1029/2000JD900110, 2000.

Wu, Z. and Reichler, T.: Variations in the Frequency of Stratospheric Sudden Warmings in CMIP5 and CMIP6 and Possible Causes, Journal of Climate, 33, 10 305–10 320, https://doi.org/10.1175/JCLI-D-20-0104.1, 2020.

Yao, W. and Jablonowski, C.: The Impact of GCM Dynamical Cores on Idealized Sudden Stratospheric Warmings and Their QBO Interactions, Journal of the Atmospheric Sciences, 73, 3397–3421, https://doi.org/10.1175/JAS-D-15-0242.1, 2016.

Yu, J.-Y. and Kim, S. T.: Relationships between Extratropical Sea Level Pressure Variations and the Central Pacific and Eastern Pacific Types of ENSO, Journal of Climate, 24, 708–720, https://doi.org/10.1175/2010JCLI3688.1, 2011.